Veterinary Immunology and Immunopathology 161 (2014) 193–204

Contents lists available at ScienceDirect

Veterinary Immunology and Immunopathology

journal homepage: www.elsevier.com/locate/vetimm

Research paper

Poly D,L-lactide-co-glycolide (PLGA) nanoparticle-encapsulated honeybee (*Apis melifera*) venom promotes clearance of *Salmonella enterica* serovar Typhimurium infection in experimentally challenged pigs through the up-regulation of T helper type 1 specific immune responses

Jin-A Lee[a,1], Bock-Gie Jung[b,1], Tae-Hoon Kim[a], Yun-Mi Kim[a], Min-Ho Park[c], Pung-mi Hyun[d], Jong-woon Jeon[d], Jin-kyu Park[d], Cheong-Weon Cho[c], Guk-Hyun Suh[e], Bong-Joo Lee[a,*]

[a] *Department of Veterinary Infectious Diseases, College of Veterinary Medicine, Chonnam National University, Gwangju 500-757, Republic of Korea*
[b] *Department of Pulmonary Immunology, University of Texas Health Science Center at Tyler, 11937 US Hwy 271, Tyler, TX 75708-3154, USA*
[c] *College of Pharmacy and Institute of Drug Research & Development, Chungnam National University, Daejeon 305-764, Republic of Korea*
[d] *Wissen Co., Ltd, #410 Bio Venture Town, 461-8, Daejeon 305-811, Republic of Korea*
[e] *Department of Veterinary Internal Medicine, College of Veterinary Medicine, Chonnam National University, Gwangju 500-757, Republic of Korea*

ARTICLE INFO

Article history:
Received 27 May 2014
Received in revised form 8 August 2014
Accepted 12 August 2014

Keywords:
Immune enhancing
PLGA
Nanoparticle
Bee venom
Melittin
Salmonella enterica serovar Typhimurium

ABSTRACT

Honeybee (*Apis melifera*) venom (HBV), which includes melittin and lipid-soluble ingredients (chrysin and pinocembrin), elicited increases in the $CD4^+/CD8^+$ T lymphocyte ratio, relative mRNA expression levels of the T helper type 1 (Th 1) cytokines (interferon-γ and IL-12) and reinforced viral clearance of an experimental porcine reproductive and respiratory syndrome (PRRS) virus infection in our previous study. On the basis of that previous study, we have now developed poly-D,L-lactide-co-glycolide (PLGA)-encapsulated HBV nanoparticles (P-HBV) for longer sustained release of HBV. We administered P-HBV to pigs *via* the rectal route, and then evaluated the potential immune-enhancing and bacterial clearance effects of P-HBV against *Salmonella enterica* serovar Typhimurium. The $CD4^+/CD8^+$ lymphocyte ratio, proliferative capacity of peripheral blood lymphocytes and relative mRNA expression levels of IFN-γ and IL-12 (produced mainly by Th1 lymphocytes) were significantly increased in the P-HBV group up to 2 weeks post-administration of P-HBV. After *S.* Typhimurium infection, the P-HBV group showed a marked reduction in microbial burden in feces and all tissue samples (including the ileum, cecum, colon, and mesenteric lymph node (MLN)), a significant increase in Th 1 cytokines (IFN-γ, IL-2, and IL-12) and a marked decrease in a Th 2 cytokine (IL-4) in

* Corresponding author. Tel.: +82 62 530 2850; fax: +82 62 530 2857.
E-mail address: bjlee@chonnam.ac.kr (B.-J. Lee).
[1] These authors contributed equally to this work.

http://dx.doi.org/10.1016/j.vetimm.2014.08.010

all tissue samples and peripheral blood lymphocytes. Thus, P-HBV may be a promising strategy for immune enhancement and prevention of *S.* Typhimurium or other bacterial infections.

1. Introduction

Salmonella enterica serovar Typhimurium (*S.* Typhimurium) is the most commonly isolated *Salmonella* serotype in pigs, and a major source of zoonotic strains of *S. enterica* responsible for human food poisoning mostly associated with the consumption of contaminated pork (Brumme et al., 2007). Typical clinical signs of *S.* Typhimurium infection in pigs are increased body temperature lasting for 2 days post infection, accompanied by diarrhea and enterocolitis (Volf et al., 2012). Pigs of all ages are susceptible to *S.* Typhimurium infection; however, weaned and growing-finishing piglets are most commonly affected and show severe clinical signs (Boyen et al., 2008). After they recover from illness, the pigs are often stunted and grow slowly, causing considerable economic losses to pig farmers (Collado-Romero et al., 2010). In addition, infected but apparently healthy pigs remain asymptomatic carriers, in which bacteria may persist without triggering any clinical signs. Such animals cannot be detected easily, and thus serve as a source of contamination (Boyen et al., 2008; Callaway et al., 2008). Therefore, *Salmonella* infection in pigs is of concern as it has an important impact on the swine industry, negatively affecting the efficiency and leading to economic losses in porcine production systems (Fosse et al., 2009).

Honeybee (*Apis melifera*) venom (HBV) has long been widely used as a traditional alternative remedy for the alleviation of pain, inflammation and some immune-related diseases such as rheumatoid arthritis and multiple sclerosis (Oršolić, 2012). Numerous studies have also reported that a component of whole HBV has several beneficial therapeutic properties, such as immune-stimulating (Son et al., 2007), anticancer (Oršolić, 2012) and radioprotective (Gajski et al., 2009) activities. HBV contains at least 18 active components, including enzymes, biogenic amines, and several biologically active peptides, including melittin (Oršolić, 2012). Melittin, the principal component extracted from the water-soluble fraction of HBV, is a well-recognized antibacterial peptide which acts rapidly and has a broad spectrum of activity against infectious agents including bacteria, fungi, viruses and parasites (Mataraci and Dosler, 2012; Liu et al., 2013). Melittin also has numerous other pharmacological effects, such as immune-stimulating and anti-cancer properties (Son et al., 2007). Hence, many commercial products containing HBV ingredients are manufactured with an emphasis on the melittin content, either as the sole index compound, or as one of a mixture of water-soluble components. The lipid-soluble fraction of HBV has received less attention from HBV manufacturers. Interestingly, some lipid-soluble components of HBV such as chrysin and pinocembrin, classified as flavonoids, have been reported to have anticancer, antioxidant and antimicrobial effects (Schnitzler et al., 2010; Rasul et al., 2013). We have previously demonstrated that our new HBV-derived product, which combines melittin, chrysin and pinocembrin enhances the $CD4^+/CD8^+$ T lymphocyte ratio, increases the relative levels of mRNA of the Th1 cytokines interferon gamma (IFN-γ) and interleukin (IL)-12, and reinforces viral clearance in pigs with experimental porcine reproductive and respiratory syndrome (PRRS) virus infection. However, these immune-enhancing effects of HBV only persisted for 7 days after HBV administration in that study. Hence, we have now developed poly-D,L-lactide-co-glycolide (PLGA)-encapsulated HBV nanoparticles (P-HBV), which are designed to achieve longer sustained release of HBV. PLGA is biocompatible, biodegradable, and is an FDA-approved agent that has been used for drug, protein, and gene delivery applications because of its sustained-release properties, which are due to the protection of entrapped materials from protease-mediated degradation (Dwivedi et al., 2013). PLGA containing hepatitis B, influenza, or PRRS viruses have been reported to effectively induce protective immune responses against several viral diseases (Thomas et al., 2011; Dwivedi et al., 2013). In addition, a study by Dube et al. (2013) demonstrated that PLGA-coated rifampicin could deliver four times rifampicin 4 times the amount of more into alveolar-like macrophages than rifampicin solution. Therefore, innovative nanotechnology using PLGA-based delivery systems could be an attractive approach for a variety of bioactive molecules, such as antibodies (Bicho et al., 2010), aptamers (Farokhzad et al., 2006), peptides (Geldenhuys et al., 2011), and prophylactic agent (Yang et al., 2013). Nanoparticle-based delivery to mucosal sites is advantageous, because nanoparticles are easily recognized and passively phagocytized by professional antigen presenting cells (APCs) (Inaba et al., 1993). Mucosal regions (ocular, nasal, oral, pulmonary, vaginal and rectal) collectively contain 80% of the body immune cells (Holmgren and Czerkinsky, 2005). Particulate antigens delivered *via* mucosal routes are recognized by microfold cells (M cells) and are then presented to APCs which strongly stimulate differentiation of T cells and effectively induce specific adaptive immune responses (Renukaradhya et al., 2012).

The aims of the current study were to (1) investigate the immune-enhancing efficacy of PLGA-encapsulated HBV delivered to pigs *via* the rectal route, and its duration period compared to non-encapsulated HBV, and (2) evaluate the bacterial clearance effect of PLGA-encapsulated HBV delivered *via* the rectal route in pigs experimentally challenged with *S.* Typhimurium, as an initial step toward using PLGA-encapsulated HBV for protection against bacterial diseases and elucidation of host cellular immune responses.

2. Materials and methods

2.1. Preparation of HBV

Crude honey bee venom (2.5 g) was obtained using a Large Quantity Bee-Venom Collector (P10-1003672, Wissen Co., Ltd., Daejeon, Korea), and was extracted with 250 ml of ultra-filtered water and 250 ml of ethyl acetate (three times each) at room temperature, and filtered through a 0.45-μm nylon membrane (Millipore, Billerica, MA, USA) under vacuum. The two filtrates were mixed and concentrated under vacuum at 40 °C. The final HBV concentrates (10 mg) were dissolved in 1 ml of ultra-filtered water and analyzed by high performance liquid chromatography (HPLC). The HBV samples used for HPLC analysis were passed through a 0.45-μm filter (Millipore) and injected into a UPLC® BEH C18 column (1.7-μm, 2.1 mm × 100 mm; Waters Corporation, Milford, MA, USA). The gradient ratios of mobile phase A (0.1% trifluoroacetic acid in methanol) and B (0.1% trifluoroacetic acid in distilled water) were 0:100 at 0–10 min at a flow rate of 0.2 ml/min, and they were kept at 50:50 at 20–30 min until finished as 100:0 at 50 min with a flow rate of 0.3 ml/min. The detection wavelength was at set 270 nm. The final HBV product was composed of 64% melittin, 3 ppm pinocembrin and 20 ppm chrysin. For use in the experiment, fine HBV powder was dissolved in a solvent consisting of 95.7% distilled water, 3.5% ethanol, and 0.8% propylene glycol (by volume) to a final concentration of 2.1 mg/ml, which was the optimal concentration determined in our preliminary experiments.

2.2. HBV-loaded PLGA nanoparticle synthesis

Nanoparticles were prepared by a standard double emulsion solvent evaporation technique (Cao and Schoichet, 1999) with some modifications. Briefly, PLGA (200 mg) was dissolved in 5 ml of dichloromethane (DCM) at room temperature. HBV (15 mg) and sucrose (5%, w/v) were dissolved in 0.5 ml of distilled water at room temperature. The two solutions were emulsified with a homogenizer for 3 min at 20,000 rpm in an ice bath, to obtain water-in-oil (W/O) emulsion. The resulting W/O emulsion was injected into 30 ml of 1.25%, w/v polyvinyl alcohol (PVA; MW 146,000–186,000) solution and homogenized for 5 min at 20,000 rpm in an ice bath, to make a water-in-oil-in-water (W/O/W) emulsion. DCM was then evaporated with stirring at room temperature overnight. The PLGA nanoparticles were isolated by centrifugation at 10,000 rpm for 30 min at 4 °C, and then washed once with 0.9% NaCl and twice with distilled water. The resulting PLGA-encapsulated HBV particles were lyophilized and stored at 4 °C prior to use. As a control, PLGA nanoparticles without HBV were prepared using the same procedure. All materials used in the nanoparticle synthesis were obtained from Sigma–Aldrich (St. Louis, MO, USA).

2.2.1. Characterization of HBV loaded PLGA nanoparticle

The size distribution and zeta potential analysis of PLGA-encapsulated HBV were performed with a laser scattering analyzer (ELS-8000, Otasuka Electronics, Osaka, Japan). Specimens were prepared by dispersion of lyophilized PLGA particles in distilled water, and then added to the sample dispersion unit and sonicated to minimize inter-particle interactions. The obscuration range was maintained between 20 and 50%. The instrument was set to measure the sample 50 times, and the average volume mean diameter was obtained. Scanning electron microscopy (SEM) was used to observe the shape of PLGA-encapsulated HBV. PLGA-encapsulated HBV was dropped onto double-sided carbon tape, then, vacuum-coated for 50 s with osmium, and examined for morphology *via* field emission SEM (JEOL JSM7500; Thermo Scientific, Rockford, IL, USA) at 3 kV accelerating voltage.

2.2.2. Determination of entrapment efficiency of HBV loaded PLGA nanoparticle

During the above preparation process, 1 ml of each supernatant was taken after centrifugation and recentrifuged at 12,000 rpm 4 °C for 10 min. The supernatants were analyzed by HPLC to measure the encapsulation efficiency (EE) and drug loading, which were calculated as follows:

$$\text{EE}\ \ (\%) = \frac{\text{Amount of the drug in the particles}}{\text{Amount of feeding drug}} \times 100$$

$$\text{Drug loading}\ \ (\%) = \frac{\text{Amount of the drug in the particles}}{\text{Amount of the particles}} \times 100$$

2.3. Animals

Conventional 4-week-old pigs were obtained from a single healthy herd without any history of *S.* Typhimurium (Daehan Livestock & Feed, Chonnam, Korea). All pigs were housed in air-conditioned rooms and allowed free access to nutritionally complete antibiotic-free pig feed and drinking water. Prior to the experiment, all pigs were tested and confirmed as *Salmonella*-free by bacteriological culture of fecal samples and biochemical characterization of isolated bacteria as previously described (Jung et al., 2012).

2.4. Experiment 1: the immune-enhancing effect of PLGA encapsulated HBV in pig

2.4.1. Experimental protocol

Pigs were randomly divided into four groups ($n = 5$ pigs per each), and administered HBV *via* the rectal route, as follows: Group 1, untreated control group; Group 2, administered only PLGA nanoparticles (PLGA group); Group 3, administered only HBV (HBV group); Group 4, administered PLGA-encapsulated HBV (P-HBV group). Blood samples were collected from all pigs prior to administration and at 7, 14 and 21 days post-administration (DPA). Body weight was monitored throughout the experimental period. All animal procedures were performed in accordance with the guidelines prescribed in the International Guiding Principles for Biomedical Research Involving Animals by the Council for International Organizations of Medical Sciences. (C.I.O.M.S., c/o WHO, Switzerland) and approved by the Institutional Animal Care and Use Committee of Chonnam National University (approval number: CNU IACUC-YB-2013-29).

Table 1
The real-time PCR primer sequences.

	Sequence (5′–3′)		Accession number[c]
TNF-α	FW[a]	CCCCCAGAAGGAAGAGTTTC	JF831365
	RV[b]	CGGGCTTATCTGAGGTTTGA	
IL-1β	FW[a]	GGCCGCCAAGATATAACTGA	NM_214055
	RV[b]	GGACCTCTGGGTATGGCTTTC	
IFN-γ	FW[a]	CAAAGCCATCAGTGAACTCATCA	X53085
	RV[b]	TCTCTGGCCTTGGAACATAGTCT	
IL-12	FW[a]	GGAGTATAAGAAGTACAGAGTGG	U08317
	RV[b]	GATGTCCCTGATGAAGAAGC	
IL-2	FW[a]	GATTTACAGTTGCTTTTGAA	X56750
	RV[b]	GTTGAGTAGATGCTTTGACA	
IL-4	FW[a]	TTGCTGCCCCAGAGAAC	AY294020
	RV[b]	TGTCAAGTCCGCTCAGG	
β-actin	FW[a]	CAGGTCATCACCATCGGCAACG	U07786
	RV[b]	GACAGCACCGTGTTGGCGTAGAGGT	

[a] FW = forward primer.
[b] RV = reverse primer.
[c] Genbank accession number of cDNA and corresponding gene available online at http://www.ncbi.nlm.nih.gov/.

2.4.2. Isolation of peripheral blood mononuclear cells

Peripheral blood mononuclear cells (PBMCs) were prepared as previously described (Jung et al., 2012). Briefly, blood samples were collected into EDTA coated tubes and diluted with equal volumes of PBS. Diluted blood was layered over half its volume of Lymphoprep (Axis-shield, Oslo, Norway) and was separated by gradient centrifugation at 800 × *g* for 30 min at room temperature. Contaminating red blood cells were lysed using Red Blood Cell Lysis Buffer Hybri-Max (Sigma–Aldrich). Lymphocytes were then washed twice with PBS and suspended in complete medium consisting of RPMI-1640 medium (Lonza, Basel, Switzerland) containing 10% (v/v) FBS (Lonza) and 2% (v/v) antibiotics–antimycotics (Lonza). Isolated cells were used for the lymphocyte proliferation assay and evaluation of T lymphocyte subpopulations.

2.4.3. Lymphocyte proliferation assays

Lymphocyte proliferation assays were conducted as previously described (Jung et al., 2013). Live lymphocytes were identified by microscopic observation of trypan blue dye (Lonza) exclusion, and counted. Cell suspensions were diluted to a final concentration of 3×10^6 cells/ml in complete medium. Cell suspensions and complete

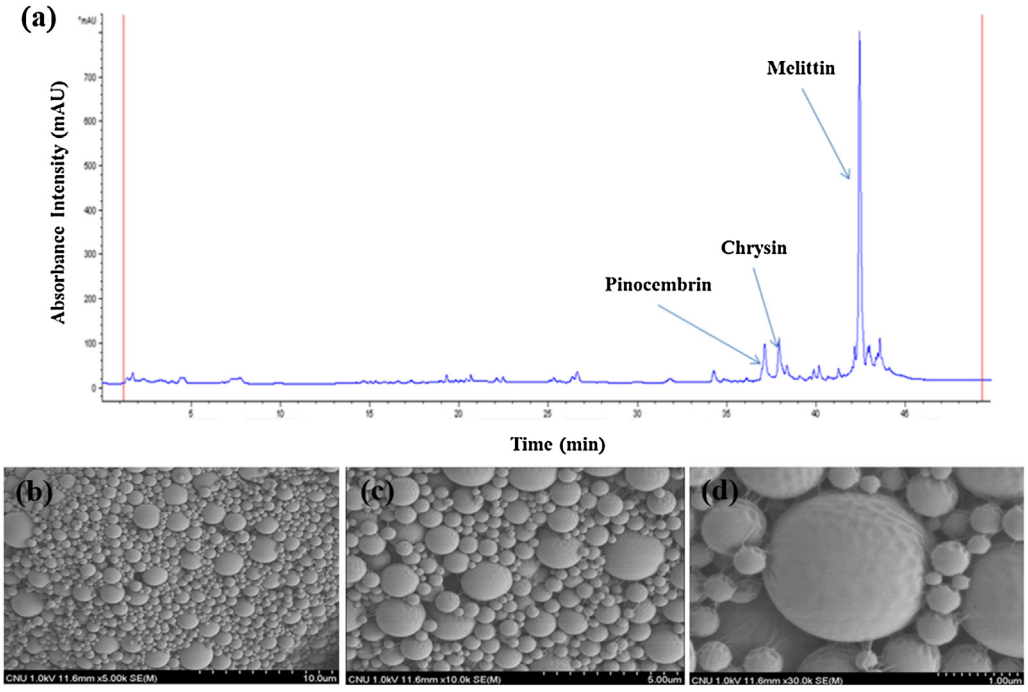

Fig. 1. (a) High performance liquid chromatography (HPLC) chemical fingerprint of honey bee venom (HBV) at 270 nm. Melittin, pinocembrin and chrysin were detected. (b) Scanning electron microscopy (SEM) images of PLGA-encapsulated HBV nanoparticles (P-HBV) with a magnification of 5000×, (c) 10,000×, and (d) 30,000×.

Table 2
Particle size, zeta potential and EE% of PLGA, and PLGA-HBV.

	PLGA	PLGA-HBV
Size (nm)	1597 ± 151.3	1780 ± 83.4
Zeta potential (mV)	−23.2 ± 8.6	−20.8 ± 3.5
EE (%)	–	96.48 ± 0.6
Drug loading (%)	–	4.86 ± 0.1

Data represents means ± standard deviation. Abbreviations: EE%, encapsulation efficiency.

medium with or without 5 μg/ml concanavalin A (Con A; Sigma–Aldrich) were added to wells of a 96-well plate in triplicate. After incubation for 48 h in a 5% CO_2 incubator at 37 °C, 20 μl of 3-(4,5-dimethylthiazol-2-yl)-2,5-diphenyltetrazolium bromide (MTT, 5 mg/ml; Sigma–Aldrich) solution was added to each well, and the plate was incubated for another 4 h. The plate was then centrifuged at 2000 × *g* for 10 min and the supernatants were discarded. A total of 200 μl dimethyl sulfoxide (DMSO; Sigma–Aldrich) was added to each well, and then plates were shaken until all formazan crystals had dissolved. The absorbance of each sample was read using a microplate spectrophotometer (Thermo Scientific) at an OD of 540 nm.

2.4.4. Evaluation of T lymphocyte subpopulation using flow cytometry

PBMC obtained from peripheral blood were analyzed to determine the $CD4^+CD8^-$ T lymphocyte and $CD4^-CD8^+$ T lymphocyte component ratios using flow cytometry as previously described (Dwivedi et al., 2013). Briefly, cells were washed with ice-cold PBS and then stained with both fluorescein isothiocyanate (FITC)-conjugated mouse anti-pig CD4 (clone 74-12-4; BD Biosciences, Franklin Lakes, NJ, USA) and phycoerythrin (PE)-conjugated mouse anti-pig CD8 (clone 76-2-11; BD Biosciences) antibodies. Respective isotype controls and unstimulated controls were also included to confirm antibody specificity and to enable correct compensation. After incubation at room temperature for 30 min in the dark, the cells were washed twice with PBS and the lymphocyte subpopulations were analyzed using a FACSCalibur flow cytometer (BD Biosciences). For calculation of $CD4^+/CD8^+$ ratio we only analyzed $CD4^{high}CD8^{low}$ cells as T helper lymphocyte and $CD4^{low}CD8^{high}$ cells as T cytotoxic lymphocyte; $CD4^{high}CD8^{high}$ double positive cells were not considered for simplicity.

2.4.5. Evaluation of cytokine mRNA expression levels in lymphocyte

The mRNA expression levels of IFN-γ, IL-2, IL-12, IL-4, TNF-α and IL-1β in lymphocytes were measured to evaluate the immune-enhancing effects of HBV and P-HBV, particularly those related to pro-inflammatory as well as Th 1 and Th 2 cytokines in the porcine immune system. Total RNA was extracted from lymphocytes using the PureLink RNA Mini Kit (Invitrogen, Grand Island, NY, USA). RNA concentration was measured using NanoDrop ND-1000 (Thermo Scientific). RNA purity was assessed by determining the ratio of the absorbance at 260 and 280 nm, and all RNA samples had 260/280 nm ratios above 1.8. Additionally, RNA integrity was confirmed by visualization of the 18S and 28S ribosomal RNA bands after electrophoresis

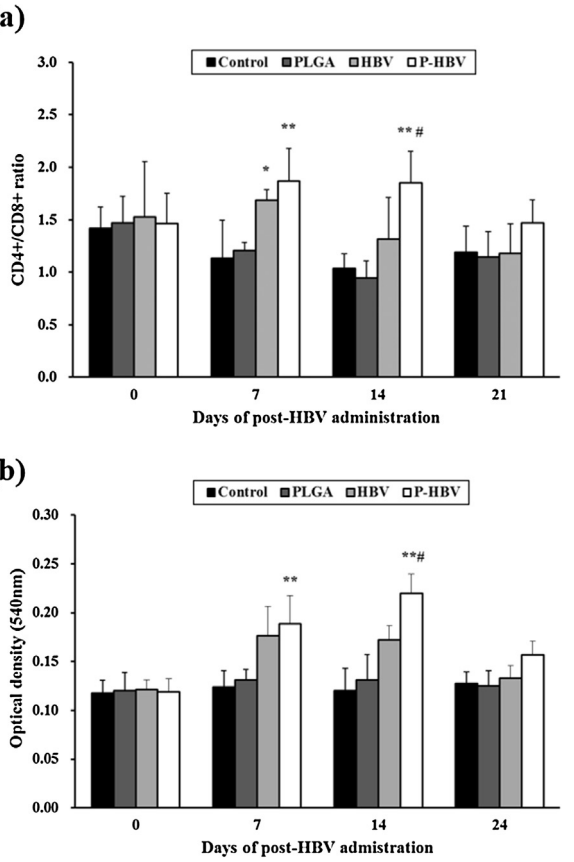

Fig. 2. Effects of PLGA-encapsulated HBV nanoparticles on T lymphocyte subpopulation ratio and lymphocyte proliferation activity in peripheral blood. HBV or P-HBV was administered *via* the rectal route. PBMCs were isolated from all pigs before administration, and 7, 14 and 21 days post-administration (DPA), and were evaluated for (a) the $CD4^+/CD8^+$ T lymphocyte ratio and (b) lymphocyte proliferation. The P-HBV group showed significant increases in $CD4^+/CD8^+$ T lymphocyte ratio and lymphocyte proliferation in comparison to the control group at 7 and 14 DPA, and also to the HBV group at 14 DPA. Values are mean ± SD (5 pigs per group). Significant differences at $^*P < 0.05$ *vs* control group, $^{**}P < 0.01$ *vs* control group, $^{\#}P < 0.05$ *vs* HBV group.

on 0.7% agarose gels (SeaKem® LE Agarose; Lonza). Equal amounts of targeted RNA were reverse-transcribed using the QuantiTect reverse transcription kit (Qiagen, Valencia, CA, USA). To minimize variations in reverse transcriptase efficiency, all samples were transcribed simultaneously. Quantitative real-time PCR was performed with iQ™ SYBR Green Supermix (Bio-Rad Laboratories, Hercules, CA, USA) using a MyiQ2 thermocycler and the SYBR Green detection system (Bio-Rad Laboratories) The real-time PCR conditions were 95 °C for 5 min, then 45 cycles of 95 °C for 30 s, 57 °C for 30 s, and 72 °C for 30 s. The primer sequences for pig IFN-γ, IL-2, IL-12, IL-4, TNF-α, IL-1β and β-actin transcripts are listed in Table 1. The threshold cycle (Ct; the cycle number at which the amount of the amplified gene of interest reaches a fixed threshold) was subsequently determined. Relative mRNA expression levels were quantified by the comparative Ct method as previously described (Livak and Schmittgen, 2001). The relative quantitation value for each target gene was normalized to an endogenous control

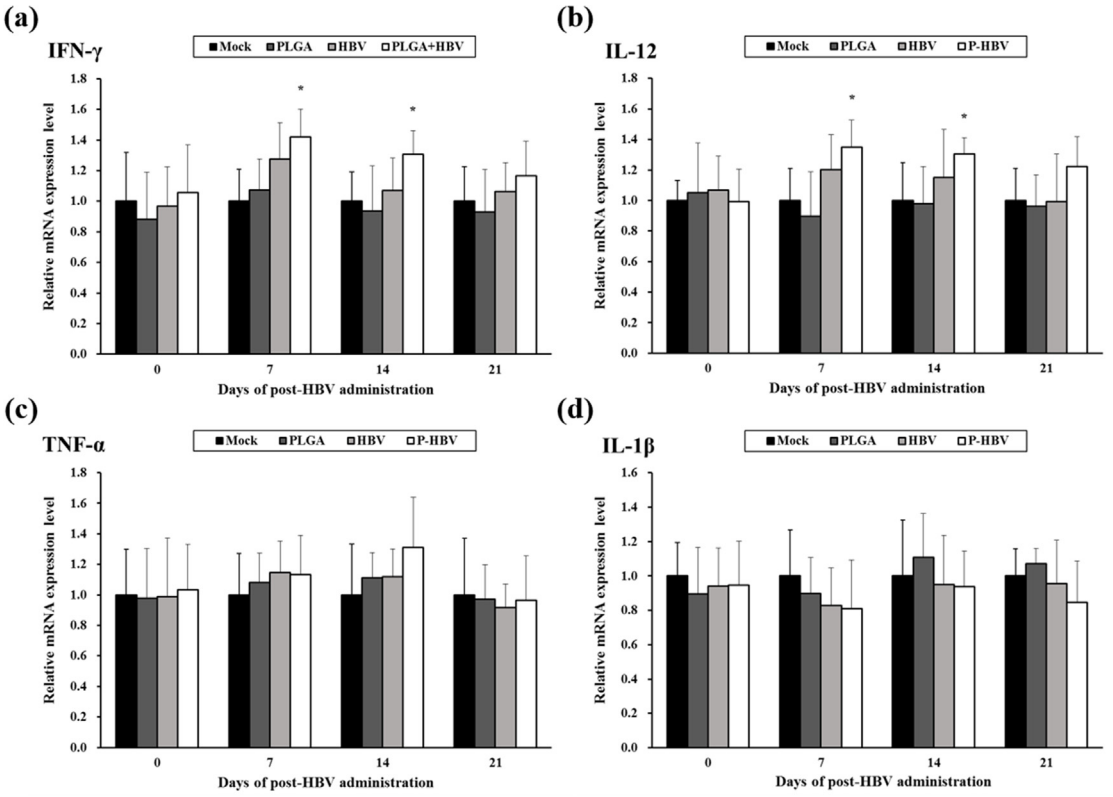

Fig. 3. Effects of PLGA-encapsulated HBV nanoparticles on the mRNA expression levels of Th 1 and pro-inflammatory cytokines in peripheral blood. The levels of (a) IFN-γ, (b) IL-12, (c) TNF-α, and (d) IL-1β in PBMCs were measured by quantitative real-time PCR. After normalization to β-actin, the data were analyzed by the Ct method. The P-HBV group showed significant increases in IFN-γ and IL-12 levels at 7 and 14 DPA compared to the control group. Values are presented as mean ± SD (5 pigs per group). Significant differences at $^{*}P < 0.05$ *vs* control group.

gene (β-actin). It was expressed as $2-\Delta\Delta$Ct (fold), where ΔCt = Ct of the target gene − Ct of the endogenous control gene and $\Delta\Delta$Ct = ΔCt of samples for the target gene – ΔCt of the target gene calibrator.

2.5. Experiment 2: microbial clearance effect of PLGA-encapsulated HBV in pigs experimentally infected with S. Typhimurium

2.5.1. Experimental S. Typhimurium infection

Pigs were randomly divided into groups, and administered either PLGA, HBV or P-HBV *via* the rectal route as described for experiment 1, and orally challenged with 10 ml of *S.* Typhimurium bacteria diluted at 1×10^9 CFU/ml, which was originally isolated from a pig with naturally occurring salmonellosis (Animal and Plant Quarantine Agency, Gyeonggi, Korea). This strain is naturally resistant to kanamycin. At the end of the experiment, all pigs were sacrificed to collect the ileum, cecum, colon and mesenteric lymph node (MLN) tissues for confirmation of bacterial clearance, and other immunological experiments. All animal procedures were performed following the guidelines of the International Guiding Principles for Biomedical Research Involving Animals by the C.I.O.M.S., and were approved by the Institutional Animal Care and Use Committee of Chonnam National University (approval number: CNU IACUC-YB-2013-29).

2.5.2. Observation of clinical signs

Each infected pig was monitored daily for typical clinical signs of salmonellosis (inappetence, depression, coughing, vomiting and diarrhea). Rectal body temperature and body weight were measured twice a day for each pig. The fecal conditions of each pig were graded at 1, 3, 5, 7 and 9 days post-infection (DPI) as previously described (Tanaka et al., 2010) with some modifications: 0 = normal feces, 1 = loose feces, 2 = mild diarrhea and 3 = severe diarrhea.

2.5.3. Viable bacterial count in fecal and tissue samples

Fecal samples were collected from each pig at 1, 3, 5, 7 and 9 DPI, and ileum, cecum, colon, and MLN samples were obtained at post-mortem examination. The samples were homogenized (10%, w/v) in PBS, and 10-fold serial dilutions were prepared. Each dilution was spread in triplicate onto XLD agar (BD Biosciences) supplemented with 100 μg/ml kanamycin, and incubated for 48 h at 37 °C. Characteristic black-colonies were counted at the dilutions where 30–300 colonies per plate were observed, and were expressed as CFU/g feces.

2.5.4. Cytokine analysis of S. Typhimurium-infected pigs

Lymphocytes were isolated from peripheral blood as described in Section 2.4.2. Total RNA extraction from lymphocytes and tissue samples (see Section 2.5.1) was performed using the TRI reagent (Molecular research

center, Cincinnati, OH, USA) and PureLink RNA Mini Kit (Invitrogen) according to the respective manufacturers' instruction. Cytokine mRNA levels were determined as described in Section 2.4.5.

2.6. Statistical analysis

The data were expressed as mean ± standard deviation (SD), and the means of different parameters were compared between groups by one-way analysis of variance (ANOVA) followed by the Tukey–Kramer multiple comparison test. All statistical analyses were performed using GraphPad InStat v. 3.0 (GraphPad Software, La Jolla, CA, USA). P values < 0.05 were considered to indicate statistical significance.

3. Results

3.1. Characterization of HBV components entrapped in PLGA nanoparticles

The HBV components pinocembrin, chrysin and melittin were detected by HPLC. The retention times of pinocembrin, chrysin and melittin are 37, 38 and 42.5 min respectively (Fig. 1a). Particle size, zeta potential, EE% and drug loading of PLGA and P-HBV are listed in Table 2. The encapsulation efficiency was 96.48 ± 0.6%, a relatively high efficiency value, and the drug loading efficiency of P-HBV was 4.86 ± 0.1%. The mean particle size of P-HBV was approximately 1780 nm. The zeta potential for P-HBV was −20.8 ± 3.5 mV. PLGA is composed of glycolic acid and lactic acid, so particles prepared using PLGA alone has negative zeta-potential. This is concordant with previous reports (Kim et al., 2008; Tahara et al., 2008; Yang et al., 2009). The external morphology of P-HBV was also observed by SEM (Fig. 1b), revealing that PLGA particles were spherical in shape, with a smooth surface. Such particles are not expected to cause any irritation to tissues, as it is known that isometric particles with smooth angles and edges cause less irritation than particles with sharp angles and edges (Malhotra and Majumdar, 2001).

3.2. Effects of PLGA-encapsulated HBV on T lymphocyte subpopulations

Flow cytometry analysis of peripheral blood was performed at days after the administration of either HBV or P-HBV. The percentage of $CD4^+CD8^-$ T lymphocytes and the $CD4^+/CD8^+$ lymphocyte ratio significantly increased after the administration of HBV or P-HBV compared to those of the control group (data not shown). In particular, the difference in the $CD4^+/CD8^+$ cell ratio was significant in the HBV group ($P < 0.05$) and the P-HBV group ($P < 0.01$) at 7 DPA compared with the control group (Fig. 2a). A significant difference from the control group was also observed at 14 DPA in the P-HBV group ($P < 0.01$), and at this time point the P-HBV group also showed a significant increase compared to the HBV group ($P < 0.05$). In the HBV group, the $CD4^+/CD8^+$ cell ratio also tended to increase, but this effect did not reach statistical significance. There were no

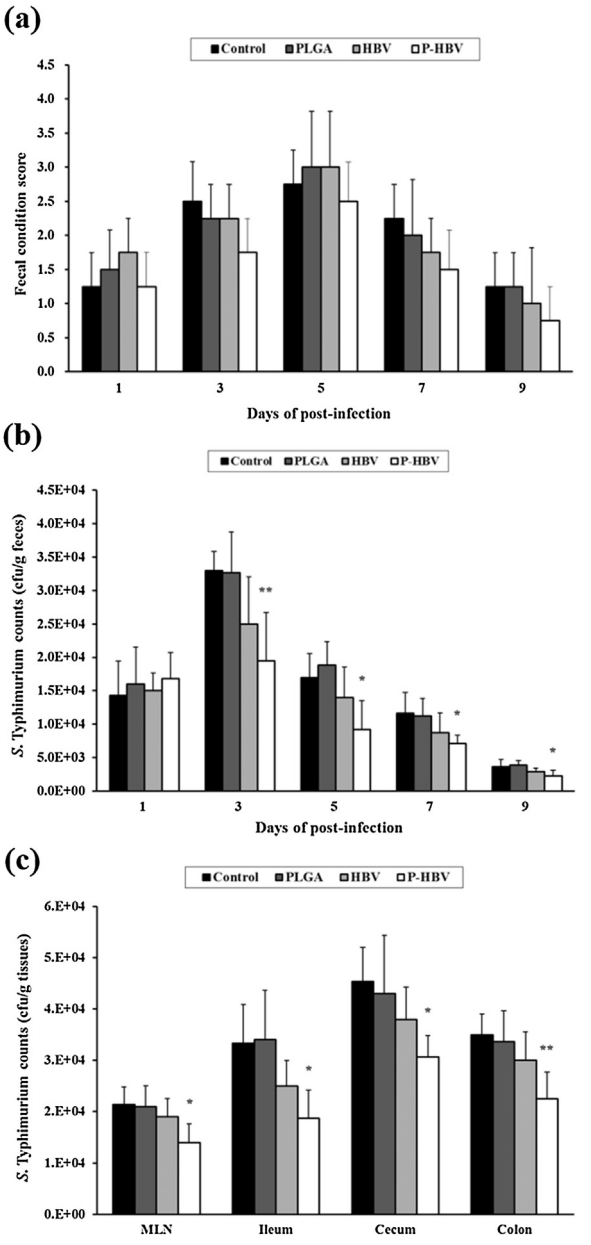

Fig. 4. Effects of PLGA-encapsulated HBV nanoparticles on *S.* Typhimurium clearance in experimentally challenged pigs. After the administration of HBV or P-HBV *via* rectal route, all pigs were orally inoculated with *S.* Typhimurium. Fecal samples were isolated from all pigs at 1, 3, 5, 7 and 9 days post infection (DPI) and used to measure (a) fecal conditioning scores and (b) fecal shedding of *S.* Typhimurium. (c) Samples of ileum, cecum, colon, and MLN tissues were collected at post-mortem examination, and the number of *S.* Typhimurium was quantified in all tissues. The P-HBV group showed a significant decrease in fecal shedding of *S.* Typhimurium at 3, 5, 7, and 9 DPI. *S.* Typhimurium counts in all investigated tissues were also markedly decreased in the P-HBV group. Values are expressed as mean ± SD (5 pigs per group). Significant differences at $^*P < 0.05$ *vs* control group, $^{**}P < 0.01$ *vs* control group.

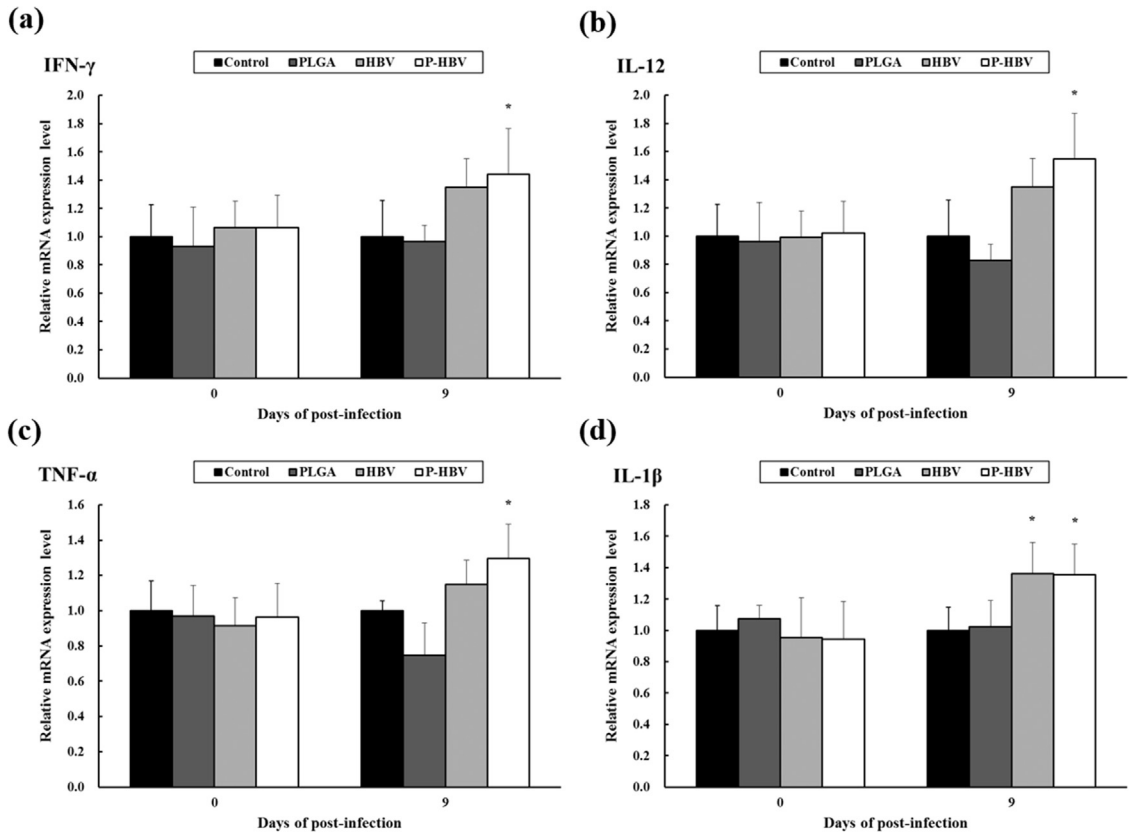

Fig. 5. Effect of PLGA-encapsulated HBV nanoparticles on the mRNA expression levels of Th 1 and pro-inflammatory cytokines in PBMC of pigs experimentally challenged with *S.* Typhimurium. PBMC were isolated from all pigs at 0 and 9 DPI, and the levels of (a) IFN-γ, (b) IL-12, (c) TNF-α, and (d) IL-1β mRNA were measured by quantitative real-time PCR analysis. After normalization to β-actin mRNA, the data were analyzed by the Ct method. The P-HBV group showed a significant increase in IFN-γ, IL-12, TNF-α, and IL-1β. Values are presented as mean ± SD (5 pigs per group). Significant differences at $^{*}P < 0.05$ *vs* control group.

significant differences between any groups at 21 DPA, and only the P-HBV group showed a slight increase.

3.3. Effects of PLGA-encapsulated HBV on lymphocyte proliferation

Lymphocyte proliferation in response to Con A was increased in both the HBV and P-HBV groups, but only the P-HBV group showed a significant increase at 7 DPA compared to the control group ($P < 0.01$). These tendencies were also observed at 14 DPA, and the P-HBV group showed a remarkable increase compared to both the control ($P < 0.01$) and HBV group ($P < 0.05$) (Fig. 2b).

3.4. Effects of PLGA-encapsulated HBV on the cytokine mRNA levels

Cytokines are the key mediators of systemic immunity, and induce several physiologically significant immune responses (Barranco et al., 2012). Thus, we analyzed representative Th 1 cytokines (IFN-γ and IL-12) and those involved in pro-inflammatory responses (TNF-α and IL-1β) after HBV or P-HBV administration. The levels of IFN-γ and IL-12 mRNA were increased after the administration of HBV or P-HBV compared to those of the control group. The P-HBV group showed significant increases in both IFN-γ and IL-12 levels compared to the control group ($P < 0.01$) at 7 and 14 DPA (Fig. 3a and b). The level of IL-12 was still higher in the P-HBV group at 21 DPA compared to the control group. The levels of TNF-α and IL-1β mRNA did not differ significantly from those of the control group in either the HBV or the P-HBV group (Fig. 3c and d).

3.5. Changes in clinical signs in S. Typhimurium-infected pigs

After experimental inoculation with *S.* Typhimurium, all pigs became infected as evidenced by the subsequent isolation of *Salmonella*. Pigs in each group showed typical clinical symptoms of salmonellosis, such as anorexia, vomiting, behavioral disturbances and diarrhea. Rectal body temperature rapidly increased to over 39.5 °C at 1–3 DPI in all groups, and no significant differences in temperature were found between the groups throughout the experimental period (data not shown). All infected animals exhibited mild diarrhea (scores of 1–2). Diarrhea symptoms became severe at 3–5 DPI (scores of 2–3), and fecal consistency generally returned to normal at 9 DPI (mostly scores of 1) (Fig. 4a). Throughout the whole experimental period, the P-HBV group showed a tendency toward lower

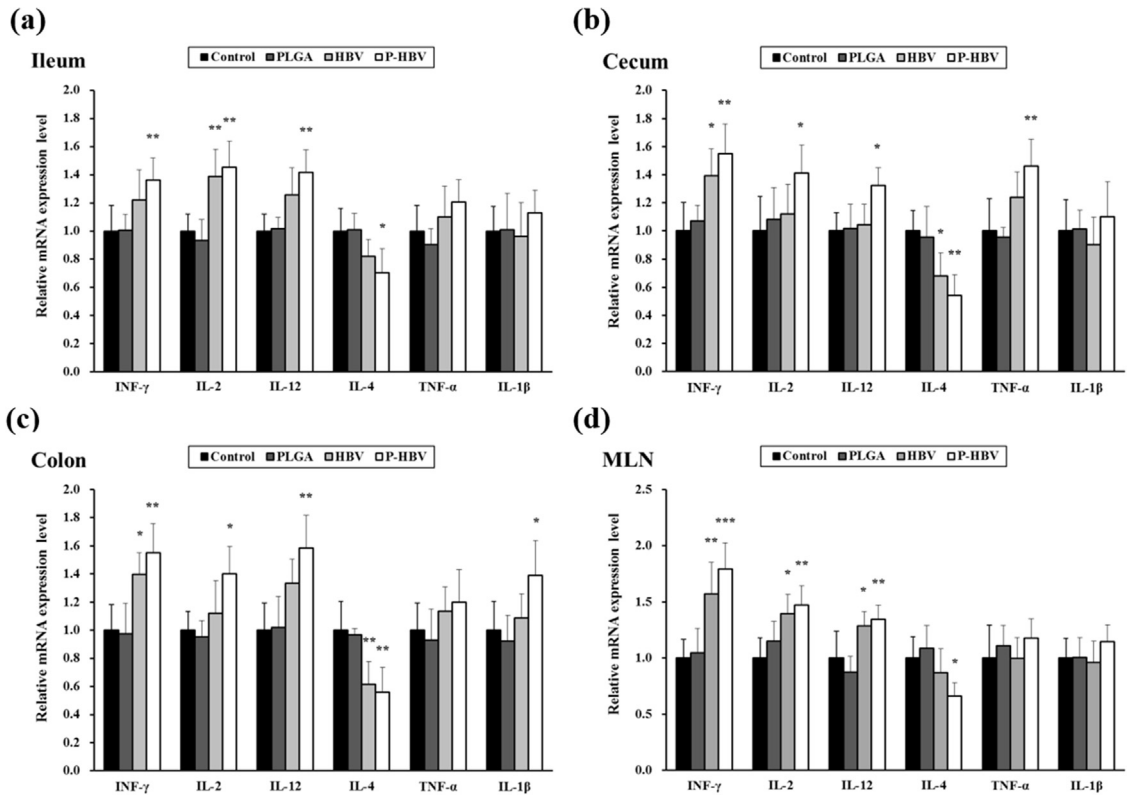

Fig. 6. Effect of PLGA-encapsulated HBV nanoparticles on the mRNA expression levels of Th 1, Th 2, and pro-inflammatory cytokines in tissues of pigs experimentally challenged with *S.* Typhimurium. (a) Ileum, (b) cecum, (c) colon and (d) MLN tissues were collected at post-mortem examination, and the levels of IFN-γ, IL-2, IL-12, IL-4, TNF-α, and IL-1β were measured by quantitative real-time PCR analysis. The P-HBV group showed a significant increase in IFN-γ, IL-2, and IL-12, and a decrease in the IL-4 in all tissues. Values are presented as mean ± SD (5 pigs per group). Significant differences at $^{*}P < 0.05$ *vs* control group, $^{**}P < 0.01$ *vs* control group.

fecal condition scores compared to all other groups, but no statistically significant differences were observed between the groups.

3.6. Bacterial clearance in the feces, ileum, cecum, colon and MLN in S. Typhimurium-infected pigs

The number of *S.* Typhimurium in the fecal samples of all infected pigs increased continuously after infection, peaked at 3 DPI, and then continuously decreased until the end of the experiment (Fig. 4b). The mean viable *S.* Typhimurium counts in the P-HBV group were significantly lower than those of the control group from 3 DPI until the end of the study ($P < 0.01$ at 3 DPI, $P < 0.05$ at 5, 7 and 9 DPI). At the end of the experiment, pathogen burdens were measured in the ileum, cecum, colon and MLN tissues.

The pathogen loads in all tissues tended to decrease in the HBV and P-HBV groups (Fig. 4c). The P-HBV group showed marked reductions of *S.* Typhimurium loads in all tissues investigated, compared to the control group ($P < 0.05$ in the ileum and cecum, $P < 0.01$ in the colon). The HBV group showed a tendency toward reduction in *S.* Typhimurium loads in all tissues, although these loads did not differ statistically significantly from the control group.

3.7. Cytokine mRNA expression profiles in S. Typhimurium-infected pigs

Levels of cytokine mRNA expression were determined in lymphocytes, and tissues affected by *S.* Typhimurium (ileum, cecum, colon and MLN). All cytokines investigated showed similar kinetic patterns (Figs. 5 and 6). In lymphocytes, the cytokine response in the P-HBV group was characterized by a significant increase in the expression of the Th1 cytokines IFN-γ and IL-12, and the pro-inflammatory cytokines TNF-α and IL-1β compared to the control group ($P < 0.05$) (Fig. 5). The HBV group also showed minor increases in IFN-γ, IL-12 and TNF-α, although these differences were not statistically significant.

In the P-HBV group, cytokine expression in the ileum in response to *Salmonella* infection was stronger than in lymphocytes, and there were marked increases in IFN-γ, IL-2 and IL-12 ($P < 0.01$), and minor increases in the pro-inflammatory cytokines TNF-α and IL-1β (Fig. 6a). The cecum and colon tissues showed patterns similar to that of the ileum (Fig. 6b and c), with the relative mRNA expression levels of IFN-γ, IL-2 and IL-12 considerably increased

in the P-HBV group compared to the control group ($P < 0.05$ for IL-2 and IL-12 in the cecum and IL-2 in the colon, $P < 0.01$ for IFN-γ in the cecum, and IFN-γ and IL-12 in the colon). However, the HBV group only showed significant increases in IFN-γ in these two tissues ($P < 0.05$). Interestingly, the P-HBV group showed marked increases in TNF-α and IL-1β in the cecum and colon respectively, unlike the expression profiles of these cytokines in the ileum. The cytokine levels in the MLN tissue were similar to those in other tissues, but the significance of the differences in the levels of IFN-γ, IL-2 and IL-12 was higher than in any other tissues (Fig. 6d). Both the HBV and P-HBV groups showed significant increases in the levels of IFN-γ, IL-2 and IL-12 ($P < 0.05$ for IL-2 and IL-12 in the HBV group; $P < 0.01$ for IFN-γ in the HBV group, and IL-2 and IL-12 in the P-HBV group; $P < 0.001$ for IFN-γ in the P-HBV group), and the P-HBV group also showed slight increases in TNF-α and IL-1β.

4. Discussion and conclusion

In the present study, we mainly evaluated the T helper (Th) lymphocyte related responses, such as the $CD4^+/CD8^+$ lymphocyte ratio, lymphocyte proliferation capacity, and expression of Th-associated cytokines, which are classically involved in cellular immune responses. Particularly, the ratio of the two main T lymphocyte subsets ($CD4^+$ cells and $CD8^+$ cells) is currently considered the most significant parameter for the evaluation of intrinsic immune responses, and high $CD4^+/CD8^+$ lymphocyte ratios are usually observed in individuals with increased immune capacity or immunofunctional ability (Xu et al., 2013). Also, stimulation of lymphocyte proliferation implies reinforced mitogenicity and immune activity of T cells (Jung et al., 2013). The $CD4^+/CD8^+$ lymphocyte ratio and relative mRNA expression levels of IFN-γ and IL-12 (which are produced mainly by Th1 lymphocytes) were significantly increased in the P-HBV group at 7 and 14 DPA compared to the control group. The proliferative capacity of PBMCs stimulated with Con A was also significantly increased in the P-HBV group. Furthermore, the P-HBV group showed a marked increase in the $CD4^+/CD8^+$ lymphocyte ratio and proliferative capacity of PBMCs at 14 DPA compared to the HBV group. These results are similar to those of our previous study, in which HBV administration led to an increase in the CD4+/CD8+ T lymphocyte ratio, and up-regulation of the levels of the Th1 cytokines, IFN-γ and IL-12; however, in that previous study, these immune-enhancing effects only lasted until 7 DPA. In contrast, in the present study the P-HBV group showed significant increases in lymphocyte proliferation and cytokine production over a 14-day period. These results imply that PLGA-entrapped HBV effectively promoted Th1 lymphocyte-specific immune responses, and these immune-enhancing effects continued until 14 days after P-HBV administration. This is similar to the results of a study by Dwivedi et al. (2013), who found that pigs vaccinated with PLGA nanoparticle-entrapped killed PRRS virus exhibited a significant increase in Th1 cytokines (IFN-γ and IL-12) and several types of immune cells, including $CD3^+CD8^+$, $CD4^+CD8^+$ and γδ T cells.

The innate immune system is composed of many different mechanisms and components, and includes a diverse array of immune cells which cooperate to achieve the rapid recognition and elimination of invading pathogens. *S.* Typhimurium has various strategies to counteract most of the host's immune defenses during different phases of infection, and subvert these immune responses (Broz et al., 2012). *S.* Typhimurium infection includes the following sequential processes: (1) localization in the intestinal lumen (2) invasion of epithelial cells, and (3) systemic dissemination to lymph nodes and organs (Martins et al., 2013). In particular, *S.* Typhimurium reaches MLN, which serve as important sites for persistence and dissemination of *Salmonella* infection (Voedisch et al., 2009). In the present study, all investigated organs (the ileum, cecum, colon and MLN) and feces exhibited the presence of *S.* Typhimurium after infection, as has been reported in other studies (Szabó et al., 2009; Calveyra et al., 2012). In addition, administration of P-HBV showed significant differences in the *S.* Typhimurium burden in the feces and the ileum, cecum, colon and MLN. These results are similar to those of a study by Calveyra et al. (2012), which showed that dietary administration of mannanoligosaccharide tended to lower fecal excretion in growing pigs. Our previous report (Jung et al., 2013) also demonstrated that HBV could increase bacterial clearance and survivability against experimental *Salmonella* Gallinarum infection in broiler chicks.

Following colonization in the intestine and MLN, *S.* Typhimurium successfully and rapidly invades host immune cells, such as macrophages, dendritic cells and neutrophils (Wick, 2004). *Salmonella* is able to persist within several immune cells by suppressing antimicrobial responses through several mechanisms, including suppression of intracellular generation of bactericidal reactive oxygen and nitrogen species, and secretion of pro-inflammatory and Th1-related cytokines such as TNF-α and IFN-γ. These cytokines are considered to be key components necessary for intracellular clearance of *Salmonella* through priming of T lymphocytes (Meurens et al., 2009). Our data demonstrated that the P-HBV nanoformulation could effectively induce production of the pro-inflammatory cytokines (TNF-α) and the Th1 cytokines (IFN-γ and IL-12) in PBMCs, most likely through the induction of gene expression. The levels of IFN-γ, IL-2 and IL-12 were also significantly increased in all investigated tissues in the P-HBV group. However, levels of the pro-inflammatory cytokines (TNF-α and IL-1β) were only significantly increased in the cecum and colon in the P-HBV group. Interestingly, IL-4 levels were significantly reduced in PBMCs and all investigated tissues. IL-4 is considered the most important differentiation cytokine for the Th 2-pathway and therefore as a suppressor of Th1-related immune responses (Brumme et al., 2007). Thus, the decreased level of IL-4 in the P-HBV group might be related to up-regulation of Th1 cytokines, such as IFN-γ, IL-2 and IL-12. These results are similar to those of our previous study (Jung et al., 2013), which showed high levels of IFN-γ and IL-18 in *S.* Gallinarum-infected broiler chicks.

In our present study, rectal delivery of PLGA-encapsulated HBV nanoparticles did not induce any toxic symptoms, and elicited much longer duration and higher efficacy of immune enhancement and microbial clearance than non-encapsulated HBV. Mucosal immunization

has several advantages over the conventional parenteral route. It can be easily performed even by untrained personnel, and optimum stimulation of mucosal immunity is very effective for protection against many infectious diseases, because it can promote both mucosal and systemic immunity (Mitragotri, 2005). The intestinal region contains various lymphoid tissues with lymphoepithelial structures involved in the induction of mucosal immune responses after uptake of particulate antigens within the intestinal tract (Mayr et al., 2012). A study by Lagranderie et al. (2002) reported that rectal immunization of newborn mice was more efficient at protecting against virulent *Mycobacterium tuberculosis* than classical subcutaneous vaccination. Furthermore, Mayr et al. (2012) demonstrated that a single rectal immunization with bacterial ghosts produced from enterohemorrhagic *Escherichia coli* (EHEC) O157:H7 fully protects mice against a 50% lethal dose (LD50) challenge with a heterologous EHEC strain; immunized mice showed significant stimulation of efficient humoral and cellular immune responses. Therefore, the immune-enhancing action of P-HBV and its effect on bacterial clearance might be related to boosting rectal mucosal immunity, which is related to the activation of Th 1-specific responses.

In conclusion, the present study demonstrated that PLGA nanoparticle-encapsulated HBV effectively enhances Th 1-specific immune responses in normal pigs, and showed better persistence than non-encapsulated HBV. During *S.* Typhimurium infection, a single rectal delivery of PLGA nanoparticle-encapsulated HBV effectively reduced microbial burden, and stimulated Th1 and pro-inflammatory responses which are known to promote bacterial clearance. Further investigations with strong emphasis on the immune mechanisms stimulated by PLGA-encapsulated HBV are needed, as the underlying mechanisms of the immune-enhancing and bacterial clearance effects of HBV are still unclear. Thus, the data presented in this study, in conjunction with further confirmation of the protective efficacy of PLGA-encapsulated HBV nanoparticles against *S.* Typhimurium infection in field studies, could lead to new strategies for immune enhancement and prevention of *S.* Typhimurium infection in the swine industry.

Acknowledgments

This study was supported by the Ministry of Agriculture, Food and Rural Affairs, Republic of Korea (project number: 311018-02-2-CG000). We would like to thank Junhwa Ji, Jaehyuk Shin, Byungchul Lee, Dongyoung Kim, Yongshuk Jung and Geunyoung Cha for their help with the animal studies. The authors have no conflicts of interests to declare.

References

Barranco, I., Gómez-Laguna, J., Rodríguez-Gómez, I.M., Quereda, J.J., Salguero, F.J., Pallarés, F.J., Carrasco, L., 2012. Immunohistochemical expression of IL-12, IL-10, IFN-α and IFN-γ in lymphoid organs of porcine reproductive and respiratory syndrome virus-infected pigs. Vet. Immunol. Immunopathol. 49, 262–271.

Bicho, A., Peca, I.N., Roque, A.C.A., Cardoso, M.M., 2010. Anti-CD8 conjugated nanoparticles to target mammalian cells expressing CD8. Int. J. Pharm. 399, 80–86.

Boyen, F., Haesebrouck, F., Maes, D., Van Immerseel, F., Ducatelle, R., Pasmans, F., 2008. Non-typhoidal *Salmonella* infections in pigs: a closer look at epidemiology, pathogenesis and control. Vet. Microbiol. 130, 1–19.

Broz, P., Ohlson, M.B., Monack, D.M., 2012. Innate immune response to *Salmonella* typhimurium, a model enteric pathogen. Gut Microbes 3, 62–70.

Brumme, S., Arnold, T., Sigmarsson, H., Lehmann, J., Scholz, H.C., Hardt, W.D., Hensel, A., Truyen, U., Roesler, U., 2007. Impact of *Salmonella* Typhimurium DT104 virulence factors *invC* and *sseD* on the onset, clinical course, colonization patterns and immune response of porcine salmonellosis. Vet. Microbiol. 124, 274–285.

Callaway, T.R., Edrington, T.R., Anderson, R.C., Byrd, J.A., Nisbet, D.J., 2008. Gastrointestinal microbial ecology and the safety of our food supply as related to *Salmonella*. J. Anim. Sci. 86, 163–172.

Calveyra, J.C., Nogueira, M.G., Kich, J.D., Biesus, L.L., Vizzotto, R., Berno, L., Coldebella, A., Lopes, L., Morés, N., Lima, G.J., Cardoso, M., 2012. Effect of organic acids and mannanoligosaccharide on excretion of *Salmonella* typhimurium in experimentally infected growing pigs. Res. Vet. Sci. 93, 46–47.

Cao, X., Schoichet, M.S., 1999. Delivering neuroactive molecules from biodegradable microspheres for application in central nervous system disorders. Biomaterials 20, 329–339.

Collado-Romero, M., Arce, C., Ramírez-Boo, M., Carvajal, A., Garrido, J.J., 2010. Quantitative analysis of the immune response upon *Salmonella* typhimurium infection along the porcine intestinal gut. Vet. Res. 41, 23.

Dube, A., Reynolds, J.L., Law, W.C., Maponga, C.C., Prasad, P.N., Morse, G.D., 2013. Multimodal nanoparticles that provide immunomodulation and intracellular drug delivery for infectious diseases. Nanomedicine, http://dx.doi.org/10.1016/j.nano.2013, pii: S1549-9634(13)00677-1.

Dwivedi, V., Manickam, C., Binjawadagi, B., Renukaradhya, G.J., 2013. PLGA nanoparticle entrapped killed porcine reproductive and respiratory syndrome virus vaccine helps in viral clearance in pigs. Vet. Microbiol. 166, 47–58.

Farokhzad, O.C., Cheng, J.J., Teply, B.A., Sherifi, I., Jon, S., Kantoff, P.W., Richie, J.P., Langer, R., 2006. Targeted nanoparticle-aptamer bioconjugates for cancer chemotherapy in vivo. PNAS 103, 6315–6320.

Fosse, J., Seegers, H., Magras, C., 2009. Prevalence and risk factors for bacterial food-borne zoonotic hazards in slaughter pigs: a review. Zoonoses Public Health 56, 429–454.

Gajski, G., Garaj-Vrhovac, V., 2009. Radioprotective effects of honeybee venom (*Apis mellifera*) against 915-MHz microwave radiation-induced DNA damage in Wistar rat lymphocytes: in vitro study. Int. J. Toxicol. 28, 88–98.

Geldenhuys, W., Mbimba, T., Bui, T., Harrison, K., Sutariya, V., 2011. Brain-targeted delivery of paclitaxel using glutathione-coated nanoparticles for brain cancers. J. Drug Target. 19, 837–845.

Holmgren, J., Czerkinsky, C., 2005. Mucosal immunity and vaccines. Nat. Med. 11, 45–53.

Inaba, K., Inaba, M., Naito, M., Steinman, R.M., 1993. Dendritic cell progenitors phagocytose particulates, including bacillus Calmette–Guerin organisms, and sensitize mice to mycobacterial antigens in vivo. J. Exp. Med. 178, 479–488.

Jung, B.G., Lee, J.A., Lee, B.J., 2012. Oxygenated drinking water enhances immune activity in pigs and increases immune responses of pigs during *Salmonella* typhimurium infection. J. Vet. Med. Sci. 74, 1651–1655.

Jung, B.G., Lee, J.A., Park, S.B., Hyun, P.M., Park, J.K., Suh, G.H., Lee, B.J., 2013. Immunoprophylactic effects of administering honeybee (*Apis melifera*) venom spray against *Salmonella* Gallinarum in broiler chicks. J. Vet. Med. Sci. 75, 1287–1295.

Kim, B.S., Kim, C.S., Lee, K.M., 2008. The intracellular uptake ability of chitosan-coated Poly (D,L-lactide-co-glycolide) nanoparticles. Arch. Pharm. Res. 31, 1050–1054.

Lagranderie, M., Balazuc, A.M., Abolhassani, M., Chavarot, P., Nahori, M.A., Thouron, F., Milon, G., Marchal, G., 2002. Development of mixed Th1/Th2 type immune response and protection against *Mycobacterium tuberculosis* after rectal or subcutaneous immunization of newborn and adult mice with *Mycobacterium bovis* BCG. Scand. J. Immunol. 55, 293–303.

Liu, H., Han, Y., Fu, H., Liu, M., Wu, J., Chen, X., Zhang, S., Chen, Y., 2013. Construction and expression of sTRAIL-melittin combining enhanced anticancer activity with antibacterial activity in *Escherichia coli*. Appl. Microbiol. Biotechnol. 97, 2877–2884.

Livak, K.J., Schmittgen, T.D., 2001. Analysis of relative gene expression data using real-time quantitative PCR and the 2(−Delta Delta C(T)) method. Methods 25, 402–408.

Malhotra, M., Majumdar, D.K., 2001. Permeation through cornea. Indian J. Exp. Biol. 39, 11–24.

Martins, R.P., Collado-Romero, M., Arce, C., Lucena, C., Carvajal, A., Garrido, J.J., 2013. Exploring the immune response of porcine mesenteric lymph nodes to *Salmonella enterica* serovar Typhimurium: an analysis of transcriptional changes, morphological alterations and pathogen burden. Comp. Immunol. Microbiol. Infect. Dis. 36, 149–160.

Mataraci, E., Dosler, S., 2012. In vitro activities of antibiotics and antimicrobial cationic peptides alone and in combination against methicillin-resistant *Staphylococcus aureus* biofilms. Antimicrob. Agents Chemother. 56, 6366–6371.

Mayr, U.B., Kudela, P., Atrasheuskaya, A., Bukin, E., Ignatyev, G., Lubitz, W., 2012. Rectal single dose immunization of mice with *Escherichia coli* O157:H7 bacterial ghosts induces efficient humoral and cellular immune responses and protects against the lethal heterologous challenge. Microb. Biotechnol. 5, 283–294.

Meurens, F., Berri, M., Auray, G., Melo, S., Levast, B., Virlogeux-Payant, I., Chevaleyre, C., Gerdts, V., Salmon, H., 2009. Early immune response following *Salmonella enterica* subspecies *enterica* serovar Typhimurium infection in porcine jejunal gut loops. Vet. Res. 40, 5.

Mitragotri, S., 2005. Immunization without needles. Nat. Rev. Immunol. 5, 905–916.

Oršolić, N., 2012. Bee venom in cancer therapy. Cancer Metastasis Rev. 31, 173–194.

Rasul, A., Millimouno, F.M., Ali Eltayb, W., Ali, M., Li, J., Li, X., 2013. Pinocembrin: a novel natural compound with versatile pharmacological and biological activities. Biomed. Res. Int. 2013, 379850, http://dx.doi.org/10.1155/2013/379850.

Renukaradhya, G.J., Dwivedi, V., Manickam, C., Binjawadagi, B., Benfield, D., 2012. Mucosal vaccines to prevent porcine reproductive and respiratory syndrome: a new perspective. Anim. Health Res. Rev. 13, 21–37.

Schnitzler, P., Neuner, A., Nolkemper, S., Zundel, C., Nowack, H., Sensch, K.H., Reichling, J., 2010. Antiviral activity and mode of action of propolis extracts and selected compounds. Phytother. Res. (Suppl. 1), S20–S28, http://dx.doi.org/10.1002/ptr.2868.

Son, D.J., Lee, J.W., Lee, Y.H., Song, H.S., Lee, C.K., Hong, J.T., 2007. Therapeutic application of anti-arthritis, pain-releasing, and anti-cancer effects of bee venom and its constituent compounds. Pharmacol. Ther. 115, 246–270.

Szabó, I., Wieler, L.H., Tedin, K., Scharek-Tedin, L., Taras, D., Hensel, A., Appel, B., Nöckler, K., 2009. Influence of a probiotic strain of *Enterococcus faecium* on *Salmonella enterica* serovar Typhimurium DT104 infection in a porcine animal infection model. Appl. Environ. Microbiol. 75, 2621–2628.

Tahara, K., Sakai, T., Yamamoto, H., Takeuchi, H., Kawashima, Y., 2008. Establishing chitosan coated PLGA nanosphere platform loaded with wide variety of nucleic acid by complexation with cationic compound for gene delivery. Int. J. Pharm. 354, 210–216.

Tanaka, T., Imai, Y., Kumagae, N., Sato, S., 2010. The effect of feeding lactic acid to *Salmonella* typhimurium experimentally infected swine. J. Vet. Med. Sci. 72, 827–831.

Thomas, C., Rawat, A., Hope-Weeks, L., Ahsan, F., 2011. Aerosolized PLA and PLGA nanoparticles enhance humoral, mucosal and cytokine responses to hepatitis B vaccine. Mol. Pharm. 8, 405–415.

Voedisch, S., Koenecke, C., David, S., Herbrand, H., Förster, R., Rhen, M., Pabst, O., 2009. Mesenteric lymph nodes confine dendritic cell-mediated dissemination of *Salmonella enterica* serovar Typhimurium and limit systemic disease in mice. Infect. Immun. 77, 3170–3180.

Volf, J., Stepanova, H., Matiasovic, J., Kyrova, K., Sisak, F., Havlickova, H., Leva, L., Faldyna, M., Rychlik, I., 2012. *Salmonella enterica* serovar Typhimurium and Enteritidis infection of pigs and cytokine signalling in palatine tonsils. Vet. Microbiol. 156, 127–135.

Wick, M.J., 2004. Living in the danger zone: innate immunity to *Salmonella*. Curr. Opin. Microbiol. 7, 51–57.

Xu, M., Zhao, M., Yang, R., Zhang, Z., Li, Y., Wang, J., 2013. Effect of dietary nucleotides on immune function in Balb/C mice. Int. Immunopharmacol. 17, 50–56.

Yang., R., Shim, W.S., Cui, F.D., Cheng, G., Han, X., Jin, Q.R., Kim, D.D., Chung, S.J., Shim, C.K., 2009. Enhanced electrostatic interaction between chitosan-modified PLGA nanoparticle and tumor. Int. J. Pharm. 371, 142–147.

Yang, S., Chen, Y., Gu, K., Dash, A., Sayre, C.L., Davies, N.M., Ho, E.A., 2013. Novel intravaginal nanomedicine for the targeted delivery of saquinavir to CD4+ immune cells. Int. J. Nanomed. 8, 2847–2858.